

Generating multi-type sequences of temporal events to improve fraud detection in game advertising

Lun Jiang, Nima Salehi Sadghiani, Zhuo Tao*

Unity

San Francisco, CA

{lun,nimas,zhuo}@unity3d.com

ABSTRACT

Fraudulent activities related to online advertising can potentially harm the trust advertisers put in advertising networks and sour the gaming experience for users. Pay-Per-Click/Install (PPC/I) advertising is one of the main revenue models in game monetization. Widespread use of the PPC/I model has led to a rise in click/install fraud events in games. The majority of traffic in ad networks is non-fraudulent, which imposes difficulties on machine learning based fraud detection systems to deal with highly skewed labels. From the ad network standpoint, user activities are multi-type sequences of temporal events consisting of event types and corresponding time intervals. Time Long Short-Term Memory (Time-LSTM) network cells have been proved effective in modeling intrinsic hidden patterns with non-uniform time intervals. In this study, we propose using a variant of Time-LSTM cells in combination with a modified version of Sequence Generative Adversarial Generative (SeqGAN) to generate artificial sequences to mimic the fraudulent user patterns in ad traffic. We also propose using a Critic network instead of Monte-Carlo (MC) roll-out in training SeqGAN to reduce computational costs. The GAN-generated sequences can be used to enhance the classification ability of event-based fraud detection classifiers. Our extensive experiments based on synthetic data have shown the trained generator has the capability to generate sequences with desired properties measured by multiple criteria.

CCS CONCEPTS

• **Computing methodologies** → **Adversarial learning**; • **Information systems** → **Computational advertising**.

KEYWORDS

Fraud detection, Temporal events, Generative adversarial network, Reinforcement learning

ACM Reference Format:

Lun Jiang, Nima Salehi Sadghiani, Zhuo Tao. 2021. Generating multi-type sequences of temporal events to improve fraud detection in game advertising.

*Authors contributed equally.

Permission to make digital or hard copies of all or part of this work for personal or classroom use is granted without fee provided that copies are not made or distributed for profit or commercial advantage and that copies bear this notice and the full citation on the first page. Copyrights for components of this work owned by others than ACM must be honored. Abstracting with credit is permitted. To copy otherwise, or republish, to post on servers or to redistribute to lists, requires prior specific permission and/or a fee. Request permissions from [permissions@acm.org](https://permissions.acm.org).

Conference'17, July 2017, Washington, DC, USA

© 2021 Association for Computing Machinery.

ACM ISBN 978-x-xxxx-xxxx-x/YY/MM...\$15.00

<https://doi.org/10.1145/nnnnnnn.nnnnnnn>

In *Proceedings of ACM Conference (Conference'17)*. ACM, New York, NY, USA, 8 pages. <https://doi.org/10.1145/nnnnnnn.nnnnnnn>

1 INTRODUCTION

Game developers can monetize their games by selling in-game ad placements to advertisers. In-game ads can be integrated to the game either through a banner in the background or commercials during breaks (when a certain part of the game is completed). There are four main elements in the game advertising ecosystem: publishers or developers, advertisers¹ (demand), advertising network, and users (supply) [21]. Game advertising networks connect advertisers with game developers and serve billions of ads to user devices triggering an enormous amount of ad events. For example, Unity Ads reports 22.9B+ monthly global ad impressions, reaching 2B+ monthly active end-users worldwide².

There are multiple types of ad events in the real-world, e.g. request, start, view, click, install, etc. Each type stands for one specific kind of ad-related user action happening at a specific time. A complete ad life cycle can be depicted as a temporal sequence of ad events, each of which is a tuple of event type with corresponding time interval. Click and install are two kinds of ad events commonly associated with ad revenue. Pay-Per-Click [17] and Pay-Per-Install [30] are the most widely used advertising models for pricing.

Naturally, as advertisers allocate more of their budgets into this ecosystem, more fraudsters tend to abuse the advertising networks and defraud advertisers of their money [22]. Fraudulent ad activities aimed at generating illegitimate ad revenues or unearned benefits are one of the major threats to these advertising models. Common types of fraudulent activities include fake impressions [14], click bots [13, 19], click farms [25], etc. [35]. Fraud in the advertising ecosystem is top of mind for advertisers, developers, and advertising networks. Having their reputation and integrity on the line, a huge amount of effort has been focused on fraud detection activities from the advertising network's side [7, 16, 21, 22].

Studying the behaviors of ads temporal sequences helps to identify intrinsic hidden patterns committed by fake or malicious users in advertising networks. Given the massive ad activity data in game advertising networks, machine learning-based approaches have become popular in the industry.

However, it is not a straightforward task to train machine learning models directly on fraudulent and benign sequences collected from ad activities [5]. The vast majority of ad traffic is non-fraudulent and data labeling by human experts is time-consuming, which results in low availability of labeled fraud sequences and a high class

¹ Advertisers can be publishers.

² <https://www.businesswire.com/news/home/20201013005191/en/>

imbalance between the fraud/non-fraud training data. Simply over-sampling the minority fraud class can cause significant overfitting while undersampling the majority non-fraud may lead to information loss and yield a tiny training dataset [1]. To mitigate this data availability problem, in this study we present a novel data generator which is able to learn the intrinsic hidden patterns from sequential training data and generate emulated sequences with high qualities.

The main contributions of our work can be summarized as follows:

- (1) We build a data generator which is able to generate multi-type temporal sequences with non-uniform time intervals.
- (2) We present a new application for event-based sequence GAN for fraud detection in game advertising.
- (3) We propose a new way of sequence GAN training by employing a Critic network.

2 RELATED WORK

Generative Adversarial Networks (GANs) [11] have drawn a significant attention as a framework for training generative models capable of producing synthetic data with desired structures and properties [18]. Ba, 2019 proposed using GANs to generate data that mimics training data as an augmented oversampling method with an application in credit card fraud. The generated data is used to assist the classification of credit card fraud [1].

Despite of the remarkable success of GANs in generating real-looking data, very few studies focus on generating sequence data. This is due to the fact that taking advantage of GAN to generate temporal sequence data with intrinsic hidden patterns can be more challenging. Recurrent Neural Network (RNN) solutions have become state-of-the-art methods on modeling sequential data. Hyland et al., 2017 developed a Recurrent Conditional GAN (RCGAN) to generate real-valued multi-dimensional time series, and then used the generated series for supervised training [9]. The time series data in their study were physiological signals sampled at specific fixed frequencies, whereas ad events data have a higher complexity in terms of non-uniform time intervals and discrete event types, and thus can not be modeled as wave signals. In ad event sequences, two events with a short time interval tend to be more correlated than events with larger time intervals.

Killoran et al., 2017 proposed a GAN-based generative model for DNA along with a activation maximization technique for DNA sequence data. Their experiments have shown that these generative techniques can learn important structure from DNA sequences and can be used to design new DNA sequences with desired properties [18]. Similar to the previous study, their focus is on the fixed interval sequences. Zheng et al., 2019 adopted the LSTM-Autoencoder to encode the benign users into a hidden space. They proposed using One-Class Adversarial Network (OCAN) for the training process of the GAN model. In their training framework, the discriminator is trained to be a classifier for distinguishing benign users and the generator produces samples that are complementary to the representations of benign users [34]. However, since OCAN has not been trained on the malicious users dataset, it is hard to measure the quality of the generated sequences and understand the pattern they follow.

2.1 Time-LSTM

The common LSTM cells have shown remarkable success to generate complex sequences with long-range structures in numerous domains [12]. Recently, a combination of a LSTM cell with a dimension-reducing symbolic representation was proposed to forecast time series [8]. However, RNN models usually consider the sequence of the events and ignore their intervals. Thus, these models are not suitable to process non-uniformly distributed events generated in continuous time. This major drawback of the traditional recurrent models has led to development of Phased-LSTM [23]. An LSTM variant to model event-based sequences. Neil et al., 2016 proposed adding a new time gate to the traditional LSTM cells. The time gate is controlled by a parametrized oscillation and has three phases, i.e. rises from 0 to 1 in the first phase, drops from 1 to 0 in the second phase, and it remains inactive in the third phase. Xiao et al., 2017 proposed using an intensity function modulated synergistically by one RNN [31]. Further, the Time-Aware LSTM (T-LSTM) cells were proposed in [2] to handle non-uniform time intervals in longitudinal patient records. They used the T-LSTM cell in an auto-encoder to learn a single representation for sequential records of patients.

Zhu et al., 2017 proposed a LSTM variant named Time-LSTM to model users' sequential actions in which LSTM cells are equipped with time gates to model time intervals [36]. In this paper, Time-LSTM was used for recommending items to users. We find it useful to model event types and time intervals using Time-LSTM cells because of its ability in capturing the intrinsic patterns of fraudulent sequences, and thus to understand the internal mechanisms of how fraudulent activities are generated. We implemented our version of Time-LSTM cells in Keras and used it in the architecture of the generators and discriminators of our GAN models.

2.2 GAN for Sequence Data

When generating continuous outputs, gradient updates can be passed from the discriminator to the generator. However, for discrete outputs, due to lack of differentiability, the backpropagation does not work properly. Yu et al., 2017 addressed the issue of training GAN models to generate sequences of discrete tokens. They proposed a sequence generation framework, called SeqGAN that models the data generator as a stochastic policy in Reinforcement Learning (RL) [32]. They regarded the generator as a stochastic parametrized policy. Their policy gradient employs MC search to approximate the state values, which is a computationally expensive process in the training loop. Moreover, the SeqGAN is limited only to discrete token generation, in our work we propose a modified version of seqGAN in combination with Time-LSTM cells that can generate both discrete tokens and continuous time intervals. To efficiently train the policy network, we employ a Critic network to approximate the return given a partially generated sequence to speed up the training process. This approach also brings the potential to use a trained Critic network for early fraud detection from partial sequences.

Zhao et al., 2020 presents an application of SeqGAN in recommendation systems. The paper solves the slow convergence and unstable RL training by using Actor-Critic algorithm instead of MC

roll-outs [33]. Their generator model produces the entire recommended sequences given the interaction history while the discriminator learns to maximize the score of ground-truth and minimize the score of generated sequences. In each step, the generator G generates a token by top-k beam search based on the model distribution. In our work, we directly sample from the distribution of the output probabilities of the tokens. While our methodologies are close, we are aiming for different goals. We optimize the generated data to solve the sample imbalance problem while they optimize for better recommendations. Therefore, different evaluation metrics are needed. Our methodologies also differ in the training strategy. For example, we used a Critic network as the baseline whereas they used Temporal-Difference bootstrap targets. They pre-trained the discriminator on the generated data to reduce the exposure bias while we pre-trained the discriminator on the actual training data for improving the metrics we use in our experiments. More importantly they do not include time intervals as an attribute in their model while we have time intervals in our models.

Recently, Smith and Smith 2020, proposed using two generators, a convolutional generator that transforms a single random vector to a RGB spectrogram image, and a second generator that receives the 2D spectrogram images and outputs a time series [28]. In our work, we find the RL training process a more natural way to address the issue of generating discrete outputs.

3 METHODOLOGY

Notation. In this paper, all sequences, sets are denoted by bold letters like \mathbf{A} . We use $|\mathbf{A}|$ to refer to the size/length of a sequences or set.

In this section, we introduce a new methodology to generate multi-type sequences using seqGAN and Time-LSTM cells.

3.1 Definitions

An original ad event sequence of length L is composed of two sub-sequences, the subsequence of event types \mathbf{x} and the subsequence of time stamps. First, we transform the time stamps \mathbf{t} into time intervals $\Delta \mathbf{t}$ and $\Delta t_m = t_m - t_{m-1}, \forall m \in [1, L]$, and $\Delta t_1 = t_1 - 0$. Then, we combine the event types and time intervals into a joint multi-type sequence \mathbf{A} :

$$\begin{aligned} \mathbf{A} = \mathbf{A}_L = \mathbf{A}_{1:L} \\ = \{(x_1, \Delta t_1), (x_2, \Delta t_2), \dots, (x_m, \Delta t_m), \dots, (x_L, \Delta t_L)\} \end{aligned} \quad (1)$$

where $\mathbf{A}_m = \mathbf{A}_{1:m}$ denotes a partial sequence from time step 1 to time step m .

3.2 Time-LSTM

In this paper, we adopt the type 1 Time-LSTM cell from [36]. The update equations of this Time-LSTM cell are as follows:

$$i_m = \sigma_i(x_m W_{xi} + h_{m-1} W_{hi} + w_{ci} \odot c_{m-1} + b_i) \quad (2)$$

$$f_m = \sigma_f(x_m W_{xf} + h_{m-1} W_{hf} + w_{cf} \odot c_{m-1} + b_f) \quad (3)$$

$$T_m = \sigma_t(x_m W_{xt} + \sigma_{\Delta t}(\Delta t_m W_{tt}) + b_t) \quad (4)$$

$$\begin{aligned} c_m = & f_m \odot c_{m-1} \\ & + i_m \odot T_m \odot \sigma_c(x_m W_{xc} + h_{m-1} W_{hc} + b_c) \end{aligned} \quad (5)$$

$$o_m = \sigma_o(x_m W_{xo} + \Delta t_m W_{to} + h_{m-1} W_{ho} + w_{co} \odot c_m + b_o) \quad (6)$$

$$h_m = o_m \odot \sigma_h(c_m) \quad (7)$$

x_m is the input feature vector at time step m , which in our case would be the embedding of the event type. Δt_m is the input time interval at time step m . i_m, f_m, T_m, o_m are the activations of input, forget, time, output gates, respectively. c_m, h_m are the cell activation and hidden state. c_{m-1} is the cell state of the previous time step ($m-1$). $\sigma_i, \sigma_f, \sigma_o$ are the sigmoid function and σ_c, σ_h are the tanh function. $W_{xi}, W_{hi}, W_{xf}, W_{hf}, W_{xt}, W_{xc}, W_{tt}, W_{xc}, W_{hc}, W_{xo}, W_{to}, W_{ho}, W_{co}$ are the weight parameters of the cell. w_{ci}, w_{cf}, w_{co} are peephole parameters.

3.3 RL and Policy improvement to train GAN

We implement a modified version of seqGAN model to generate multi-type temporal sequences. Time-LSTM cells are utilized in our implementations for both the generator G and the discriminator D .

The sequence generation process of our generator G can be modeled as a sequential decision process in RL. The state at time step m is defined as:

$$S_m = [T_m(\mathbf{A}_m, \theta); h_m(\mathbf{A}_m, \theta)] \quad (8)$$

where T_m is the time gate activate in (4) and h_m is the hidden state in (7). \mathbf{A}_m is the partial sequence at time step m and θ is the trainable parameters of the Time-LSTM cell.

The action at time step m is a combination of two parts: $a_m = \{a_m^x, a_m^{\Delta t}\}$, where a_m^x is the action to find the next event type x_{m+1} and $a_m^{\Delta t}$ is the action to find the next time interval Δt_{m+1} . Thus a new partial sequence \mathbf{A}_{m+1} can be formed step by step, until a complete sequence $\mathbf{A} = \mathbf{A}_L$ of length L described in (1) is constructed.

To make decisions in this sequence generation process, we employ a hybrid policy to represent action spaces with both continuous and discrete dimensions (similar to the idea in [24]). This policy is designed to choose discrete event types and continuous time intervals, assuming their action spaces are independent. Then we use a categorical distribution and a Gaussian distribution to model the policy distributions for the event types and the time intervals respectively. So the hybrid generator policy can be defined as:

$$\begin{aligned} G_\theta(a_m|S_m) &= \pi_\theta^x(a_m^x|S_m) \cdot \pi_\theta^{\Delta t}(a_m^{\Delta t}|S_m) \\ &= \text{Cat}(x|\alpha_\theta(S_m)) \cdot \mathcal{N}(\Delta t|\mu_\theta(S_m), \sigma_\theta^2(S_m)) \end{aligned} \quad (9)$$

where $x \in \mathbf{K}, \Delta t \in \mathbf{R}_{\geq 0}$. \mathbf{K} is the set of all possible event types.

When generating a new event type and time interval at each step, we follow the generator policy and sample from categorical and normal distributions independently and concatenate them to obtain the action vector a_m , then append them to the current partial sequence \mathbf{A}_m to obtain a new partial sequence \mathbf{A}_{m+1} . Once a

complete sequence of length L has been generated, we pass the sequence \mathbf{A} to the Discriminator D which predicts the probability of the sequence to be real against generated:

$$D_\phi(\mathbf{A}) = \Pr(Y = 1 | \mathbf{A}; \phi) \quad (10)$$

The feedback from D can be used in training G such that G can better learn how to generate sequences similar to real training data to deceive D . Because the discrete data is not differentiable, gradients can not passed back to generator like in image-base GANs.

The original seqGAN training uses Policy Gradient method with Monte-Carlo roll-out to optimize the policy.[32]. In order to reduce variance in the optimization process, seqGAN runs the roll-out policy starting from current state till the end of the sequence for multiple times to get the mean return. Here we use an Actor-Critic method with a Critic network instead of MC roll-out to estimate the value of any state, which is computationally more efficient.[3].

The Critic network models a state-dependent value $\hat{V}_\psi^{G_\theta}(S_m)$ for a partially generated sequence A_m under policy G_θ , which is defined as the expected future return for a complete sequence provided by the Discriminator D :

$$\hat{V}_\psi^{G_\theta}(S_m) = \mathbb{E}_{\mathbf{A}_{m+1:L} \sim G_\theta(S_m)} [D_\phi(\mathbf{A})] \quad (11)$$

The value function parameters are updated during training by minimizing the mean squared error between the true return $D_\phi(\mathbf{A})$ and the value function $\hat{V}_\psi^{G_\theta}(S_m)$:

$$J(\psi) = \mathbb{E}[(D_\phi(\mathbf{A}) - \hat{V}_\psi^{G_\theta}(S_m))^2] \quad (12)$$

The difference between them, $D_\phi(\mathbf{A}) - \hat{V}_\psi^{G_\theta}(S_m)$, is named the advantage function, which is used in G training and helps to reduce variance.

The goal of G training is to choose actions based on a policy that maximizes expected return. The object function of G follows Policy Gradient method [29] which can be derived as:

$$\nabla_\theta J(\theta) = \sum_{m=0}^{L-1} \mathbb{E}_{a_m \sim G_\theta(a_m | S_m)} [\nabla_\theta \log G_\theta(a_m | S_m) \cdot (D_\phi(\mathbf{A}) - \hat{V}_\psi^{G_\theta}(S_m))] \quad (13)$$

Because of the independence assumption we made, the policy gradient term can be broken down and written into a categorical cross-entropy and a Gaussian log-likelihood as follows:

$$\begin{aligned} & \nabla_\theta \log G_\theta(a_m | S_m) \\ &= \nabla_\theta [\log \text{Cat}(x | \alpha_\theta(S_m)) + \log \mathcal{N}(\Delta t | \mu_\theta(S_m), \sigma_\theta^2(S_m))] \\ &= \nabla_\theta [\mathbb{E}_{x' \in \mathcal{K}} \mathbb{1}_{x'}(x) \Pr(x = x') \\ & \quad - \frac{(\Delta t - \mu_\theta(S_m))^2}{2\sigma_\theta^2(S_m)} - \frac{1}{2} \log(2\pi\sigma_\theta^2(S_m))] \end{aligned} \quad (14)$$

The goal of D training to use distinguish generated sequences with true sequences from training data.³ D_ϕ is updated through minimizing binary cross-entropy loss.

We keep training G and D alternatively. The Pseudo code of the entire process is shown in Algorithm 1.

Algorithm 1 Sequence Generative Adversarial Nets

Require: generator policy G_θ ; Critic $\hat{V}_\psi^{G_\theta}$; discriminator D_ϕ ; positive dataset $\Omega^+ = \{\mathbf{A}_{1:L}^+\}$, negative dataset $\Omega^- = \{\mathbf{A}_{1:L}^-\}$

- 1: Initialize $G_\theta, D_\phi, \hat{V}_\psi^{G_\theta}$ with random weights θ, ϕ, ψ
- 2: Pre-train G_θ using MLE on $\Omega^+ \cup \Omega^-$.
- 3: Pre-train D_ϕ via minimizing binary cross-entropy on $\Omega^+ \cup \Omega^-$
- 4: **repeat**
- 5: **for** G -steps **do**
- 6: Generate a batch of complete sequences $\mathbf{A} \sim G_\theta$
- 7: Get total rewards $D_\phi(\mathbf{A})$ from discriminator
- 8: $x_0 \leftarrow$ initial token
- 9: $\Delta t_0 \leftarrow 0$
- 10: **for** m in $0 : L - 1$ **do**
- 11: Calculate current state S_m via Eq. (8)
- 12: Sample $x_{m+1} \sim \text{Cat}(x | \alpha_\theta(S_m))$
- 13: Sample $\Delta t_{m+1} \sim \mathcal{N}(\Delta t | \mu_\theta(S_m), \sigma_\theta^2(S_m))$
- 14: Compute value estimate from Critic $\hat{V}_\psi^{G_\theta}(S_m)$
- 15: Compute the advantage $(D_\phi(\mathbf{A}) - \hat{V}_\psi^{G_\theta}(S_m))$
- 16: **end for**
- 17: Update Critic param. ψ by minimizing Eq. (12)
- 18: Update generator param. θ via policy gradient Eq. (13)
- 19: **end for**
- 20: **for** D -steps **do**
- 21: Generate a batch of sequences $\mathbf{A}_{fake} \sim G_\theta$
- 22: Sample a batch of sequences \mathbf{A}_{true} from Ω^+
- 23: Train discriminator D_ϕ on $\mathbf{A}_{fake} \cup \mathbf{A}_{true}$ and update param. ϕ via minimizing binary cross-entropy
- 24: **end for**
- 25: **until** terminate condition satisfied

4 DATA EXPERIMENTS

Due to the concerns about data privacy laws (e.g. GDPR⁴, CCPA⁵), and to protect confidential details of the Unity Fraud Detection service, we decide not to use real-world ad events data and patterns for this study, thus to avoid data privacy issues and prevent fraudsters from reverse-engineering the presented algorithms and rules to circumvent fraud detection systems. Instead, we conduct our experiments on a synthetic dataset emulating real-world ad events.

4.1 Synthetic Dataset

We define the synthetic dataset as Ω , and 6 types of events $\mathcal{K} = \{a, b, c, d, \text{PAD}, \text{INI}\}$ where $\mathcal{K}' = \{a, b, c, d\}$ is the set of hypothetical ad event types; PAD is reserved for padding and end token; INI is the dummy initial token marking the beginning of a sequence, which always comes with a zero initial time interval.

Each sequence in the synthetic dataset has a uniform length $L = 21$, including the dummy initial step $(x_0, \Delta t_0) = (\text{INI}, 0)$. For the following steps, each event type x_m is randomly sampled from \mathcal{K}' with an equal probability, and each time interval Δt_m is sampled from a Chi-Square distribution with the degree of freedom

³Definitions of the training data, positive and negative datasets are in section 4.1

⁴General Data Protection Regulation

⁵California Consumer Privacy Act

conditioned on x_m , i.e.:

$$x_m \sim \text{Uniform}\{a, b, c, d\} \quad (15)$$

$$\Delta t_m \sim \chi^2(k), \quad k = \begin{cases} 8 & \text{if } x_m = a \\ 16 & \text{if } x_m = b \\ 24 & \text{if } x_m = c \\ 32 & \text{if } x_m = d \end{cases} \quad (16)$$

One example of a complete synthetic sequence is as below:

$$\begin{aligned} A_{e.g.} = & [(INL, 0), (d, 28), (a, 6), (a, 3), (c, 18), (c, 32), (a, 15), \\ & (c, 26), (c, 27), (a, 11), (a, 3), (a, 7), (a, 10), (d, 26), \\ & (b, 8), (c, 24), (d, 22), (a, 6), (d, 39), (d, 19), (c, 21)] \end{aligned}$$

Then, we split the synthetic dataset Ω into a positive dataset Ω^+ and a negative dataset Ω^- , by a set of human defined rules. These rules are variants of real-world rules observed in ad activities. In this study, we intentionally avoid using real patterns or rules that appear in real fraud detection work, in order to prevent potential information leakage to fraudsters.

There rules we defined are as follows:

- (1) A sequence starts with an a event.
- (2) There are more than three distinct types of events after the initial token, and at least one of them is a .
- (3) Each d event is paired with one and only one previous c event. Each c event can be paired with at most one later d event.
- (4) The total number of a events is greater or equal to that of b events; The total number of b events is greater or equal to that of c events; The total number of c events is greater or equal to that of d events.
- (5) The time delay between any two consecutive same events is no smaller than 10
- (6) The time delay between any two paired c and d events is no greater than 50.

If a sequence follows more than three rules out of six, it is classified as a positive sequence $A^+ \in \Omega^+$, otherwise as a negative sequence $A^- \in \Omega^-$.

The goal of GAN training is to teach the generator D_θ to learn the intrinsic human-defined patterns in the synthetic dataset Ω , and generate sequences satisfying as many above-mentioned rules as possible. In a real-world application, those patterns can be hidden or unknown to human experts, but a GAN is expected to learn and reproduce the patterns that are not intuitive to humans.

4.2 Evaluation Metric

In the last few years, several different evaluation metrics for GANs have been introduced in the literature. Among them, Fréchet Inception Distance (FID) [15] has been used extensively [6]. However, it is not enough to show the effectiveness of our training on multi-type sequences using only one metric. This is due to the fact that our sequences consist of a discrete categorical part (event type) and a continuous numerical part (time interval). We propose using multiple metrics including a Rule-Based Quality (RBQ) score (to check if the sequences follow our validity rules), Mean Absolute Deviation (MAD) metric (event types are diverse), and Maximum Mean Discrepancy (MMD) [10] (dissimilarity between event types

or time intervals) in addition to FID for time intervals. The arrows (\uparrow / \downarrow) show the improvement directions.

RBQ \uparrow . The quality of a generated sequence is measured by a metric derived from the six rules we defined in section 4.1. The general intuition behind the RBQ score is that it is less probable for a generated sequence to follow multiple human-defined rules, so that a sequence with more desired patterns deserves a higher quality score. As a result, in RBQ, rule combinations are weighted by their length, where an individual rule is considered as a combination of length 1. The six rules are considered equally important in calculation. We employ a geometric series with common ratio 2 for weighting. The RBQ score for a sequence A is defined as follows:

$$RBQ(A) = \sum_{\lambda \in \Lambda(A)} 2^{|\lambda|} \quad (17)$$

where $\Lambda(A)$ is the set of all rule combinations that sequence A follows, λ is one rule combination, and $|\lambda|$ is its length. For example, if a sequences follow rule 1 and rule 2 described in section 4.1, then it contains 3 different rule combinations $\{1, 2, (1, 2)\}$, thus yields an RBQ score of $2 + 2 + 2^2 = 8$.

MAD \uparrow . We propose using MAD to measure statistical dispersion of the categorical part of the multi-type sequences, i.e., the event types. We use dispersion as a proxy for diversity of the generated event types. Basically, we one-hot encode the event types and compute the mean absolute deviation of each sequence from the median of all sequences. Median is known to be more robust to noise and fits our need to have categorical values as opposed to mean. Given the diversity oracle, we compare the MAD score of any batches of sequences against the MAD score of a batch of sampled sequences from our Ω^+ dataset as the comparison base. MAD can be computed using:

$$MAD(B) = \frac{1}{|B|} \sum_{A \in B} \sum_{m=1}^L |x_m^A - \tilde{E}_m(B)| \quad (18)$$

where B is a batch of sequences, $|B|$ is the batch size, A is a sequence of length L in B , x_m^A is the event type of step m in A , $\tilde{E}_m(B)$ is the median of the event types at step m across the batch B .

FID \downarrow . We use FID to evaluate the numerical part of the multi-type sequences, i.e., the time intervals. It focuses on capturing certain desirable properties including the quality and diversity of the generated sequences. FID performs well in terms of robustness and computational efficiency [4]. The Fréchet distance between two Gaussians is defined as:

$$FID(x, g) = \|\mu_x - \mu_g\|_2^2 + \text{Tr} \left(\Sigma_x + \Sigma_g - 2(\Sigma_x \Sigma_g)^{\frac{1}{2}} \right) \quad (19)$$

where (μ_x, Σ_x) and (μ_g, Σ_g) are the means and covariances of the samples from the real data distribution and model distribution, respectively.

MMD \downarrow . We also employ MMD to evaluate the time intervals. This measure computes the dissimilarity between two probability distributions P_r and P_g using samples drawn independently from each. We use an estimator with Radial Basis Function (RBF) kernel

k , which is:

$$\begin{aligned} \text{MMD}_k(X, Y) = & \frac{1}{\binom{n}{2}} \sum_{i \neq i'} k(\mathbf{x}_i, \mathbf{x}_{i'}) - \sum_{i \neq j} \frac{2}{\binom{n}{2}} k(\mathbf{x}_i, \mathbf{y}_j) \\ & + \frac{1}{\binom{n}{2}} \sum_{j \neq j'} k(\mathbf{y}_j, \mathbf{y}_{j'}) \end{aligned} \quad (20)$$

FIDH ↓. This metric is a variant of FID, which views the Time-LSTM hidden state $[T_m(\phi); h_m(\phi)]$ in $D_\phi(\mathbf{A})$ as a continuous multivariate Gaussian distribution. Then the FID score will be computed between two hidden states using Eq. 19. Hidden states can be viewed as representations of the input sequence. FIDH uses the information from both the discrete part and the continuous part of our multi-typer sequence.

4.3 Experiment Setup

We use the Ω^+ and Ω^- datasets defined in section 4.1 for model training and evaluation. Both datasets contain around 150000 data samples. As described in Algorithm 1, we first pre-train G and D until convergence, and then start RL training for the pre-trained G and D . In this section, we compare the generated sequences from the following models:

- G0: Generator with initial random model parameters.
- G1: Generator pre-trained using MLE.
- G2: Generator trained by algorithm 1.

We monitor the training process and use the metrics defined in section 4.2 to evaluate model performance during training, which are plotted in Figure 1. The ratio between G -steps and D -steps is

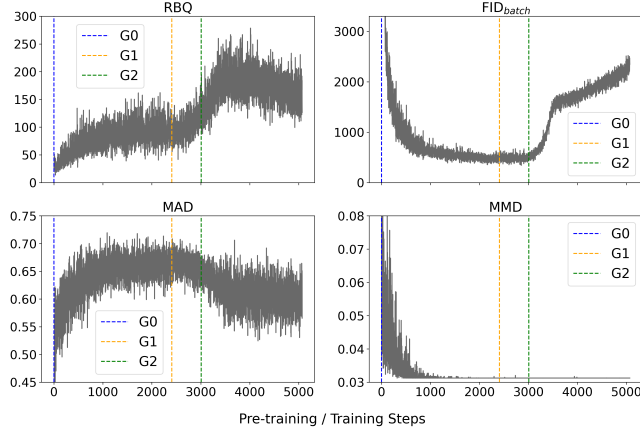


Figure 1: Performance metrics calculated during the training process.

set to 1 : 1. Both G and D have the same batch size 64, and use the SGD optimizer with learning rate 10^{-4} . We save the models during the training process and present the best performed models for evaluation.

As shown in Figure 1, G0 is the randomly initialized model (blue line), G1 is the model pre-trained by MLE after 2400 steps (orange line), and G2 is the generator which is trained for 3000 steps (green line) using algorithm 1. During the pre-training process, RBQ and MAD increase, while FID and MMD decrease. After the

Table 1: Oracle metrics calculated using Ω^+ as base

Samp.	RBQ ↑	MAD ↑	FID ↓	MMD ↓	FIDH ↓
G0	14.7290	1.1114	9719.9854	0.1563	5.4784
G1	81.0501	1.3208	103.7343	0.0002	3.3819
G2	123.5881	1.2503	187.6541	0.0002	2.6775
Ω^+	122.1438	1.2880	0.0000	0.0000	—
Ω^-	12.2944	1.4534	64.6673	0.0002	—

pre-training finishes and RL training starts, RBQ keeps increasing, and FID surges dramatically after certain point (3000 steps in Figure 1), where we stop training because it indicates a mode-collapsed generator. Notably, the FID score measured in training process is calculated between the training batch sampled from Ω^+ and the evaluation batch generated by G , both of size 64, which is different from the FID and FIDH scores in Table 1.

4.4 Experiment Results

To evaluate the performance of a generator after training, we use the trained generator to create test datasets. Each model generates 30 batches of size 10000. Then, we performed a two-sample t-test to compare each test dataset with samples of the same size drawn from Ω^+ and Ω^- .

Oracle scores. The Tables 1 show the **mean** values of the different metrics over 30 batches. In particular, the MAD, FID score and FID score for hidden units (FIDH) are calculated respectively using data sampled from Ω^+ as the base for the comparisons. The results are presented in 1. The results demonstrate that the sequences generated by G2 network have a significantly higher RBQ score than that generated by MLE pre-trained generator G1 and randomly initialized generator G0. The RBQ score of G2 is close to the samples drawn from Ω^+ , which shows the high quality of these sequences. It indicates the generator G2 is able to learn the intrinsic patterns and rules in Ω^+ during RL-training, and then generate sequences that mimics these patterns to deceive the discriminator.

From the perspective of FID and MAD, G2 has lower scores compared to the MLE pre-trained generator G1. As we discussed, in section 4.2, FID evaluates the continuous distribution of the time interval Δt , and MAD measures the dispersion of the discrete event type x in a sequence. In each sequence from the training datasets, the two features are intrinsically correlated. However, FID only evaluates the continuous part of the sequences and MAD evaluates the discrete part of the sequences separately as two independent distributions without paying attention to their internal correlations. As a result, although G1 have a higher FID score for time intervals and higher MAD score for event types, it has a lower RBQ score compared to G2. This is because the RBQ score is calculated based on the joint distribution of time intervals and event types. Same logic applies to FIDH score as well, G1 has a lower FIDH score than G2, because FIDH is calculated between the hidden state representations of two sequences, which utilizes the information from both time intervals and event types. Moreover, MMD converges fast during the training and both G1 and G2 have very similar performance with regards to MMD.

4.5 Discussion

Most metrics such as FID only yield one-dimensional scores and fail to distinguish between different failure cases. Given that in Table 1 both $G1$ and $G2$ have similar performances, we propose using Precision and Recall for Distributions (PRD) [27] to explain their differences. PRD is used to compare a distribution Q to a reference distribution P . The intuition behind PRD is that precision measures how much of Q can be generated by P while recall measures how much of P can be generated by Q . Figure 2 illustrates the comparison of the PRD curves among $G0$, $G1$, and $G2$: We can interpret the

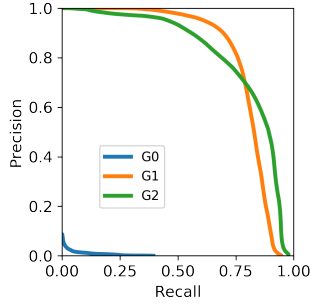


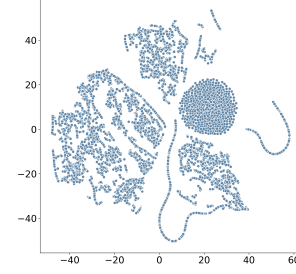
Figure 2: Comparison of PRD curves of $G0$, $G1$, and $G2$

differences between $G1$ and $G2$ from Figure 2: for a desired recall level of ~ 0.8 and lower, $G1$ generates sequences closer to the training data. However, if one desires a recall higher than ~ 0.8 , $G2$ enjoys higher precision.

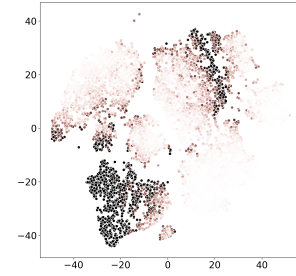
We next examine the representations learned by the discriminator that underpinned the successful performance of it. We use t-SNE [20] to visualize the output of the Time-LSTM cell. Basically, the nearby points in the representation space have similar rewards given by the discriminator.

We generate 10000 sequences from each of $G0$, $G1$, and $G2$ and pass them to the discriminators that trained with the corresponding generators. Figure 3 depicts the two-dimensional t-SNE embedding of the representations of the outputs of the Time-LSTM cells for each discriminator. The points are colored according to the predicted rewards from the discriminator. Darker colors mean higher reward. We can clearly see in Figure 3, discriminator $D2$ has more points with relatively darker colors than discriminators $D1$ and $D0$, which means the discriminator that is trained with $G2$ returns higher rewards for the generated sequences. On the other hand, the discriminator $D0$ seems to return a mean value for all the sequences (same color). This is due to the fact that $D0$ is a randomly initialized discriminator. The t-SNE embeddings can be also used for feature extraction on labeled data.

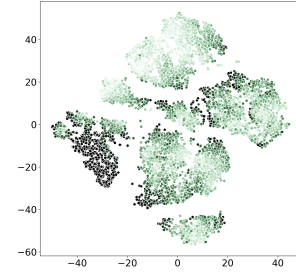
Radford et al., 2015 has shown a way to build high quality representations by training a GAN model and reusing parts of the generator and discriminator networks as feature extractors for other supervised tasks [26]. This can be potentially a promising future direction for this work.



(a) $D0$



(b) $D1$



(c) $D2$

Figure 3: Two-dimensional t-SNE embedding of the representations of the outputs of Time-LSTM cells

5 CONCLUSIONS

In this paper, we have described, trained, and evaluated a seqGAN methodology for generating artificial sequences to mimic the fraudulent user patterns in ad traffic. We have additionally employed a variant of Time-LSTM cell to generate synthetic ad events with non-uniform time intervals between events. As this task poses new challenges, we have presented a new solution by training seqGAN using a combination of MLE pre-training and a Critic network. The generator proposed in this paper is capable of generating multi-type temporal sequences with non-uniform time intervals, which is one of the novelties of our developed methodology. We have also

proposed using multiple criteria to measure the quality and diversity of the generated sequences. Through numerous experiments, we have discovered that the generated multi-type sequences are of desired properties.

Furthermore, we compared the performance of our generator under different settings with randomly sampled data from our training datasets. We concluded that the seqGAN-trained generator has a higher performance compared to pre-trained generators using MLE, measured by multiple criteria including RBQ and FIDH scores that are appropriate for evaluating multi-type sequences.

6 ACKNOWLEDGMENTS

The authors would like to thank Unity for giving the opportunity to work on this project during Unity's HackWeek 2020.

REFERENCES

- [1] Hung Ba. 2019. Improving Detection of Credit Card Fraudulent Transactions using Generative Adversarial Networks. *arXiv preprint arXiv:1907.03355* (2019).
- [2] Inci M Baytas, Cao Xiao, Xi Zhang, Fei Wang, Anil K Jain, and Jiayu Zhou. 2017. Patient subtyping via time-aware lstm networks. In *Proceedings of the 23rd ACM SIGKDD international conference on knowledge discovery and data mining*. 65–74.
- [3] Shalabh Bhatnagar, Richard S Sutton, Mohammad Ghavamzadeh, and Mark Lee. 2007. Naturalgradient actor-critic algorithms. *Automatica* (2007).
- [4] Ali Borji. 2019. Pros and cons of gan evaluation measures. *Computer Vision and Image Understanding* 179 (2019), 41–65.
- [5] Jin-A Choi and Kiho Lim. 2020. Identifying machine learning techniques for classification of target advertising. *ICT Express* (2020).
- [6] Terrance DeVries, Adriana Romero, Luis Pineda, Graham W Taylor, and Michal Drozdal. 2019. On the evaluation of conditional GANs. *arXiv preprint arXiv:1907.08175* (2019).
- [7] Feng Dong, Haoyu Wang, Li Li, Yao Guo, Tegawendé F Bissyandé, Tianming Liu, Guoai Xu, and Jacques Klein. 2018. Fraudroid: Automated ad fraud detection for android apps. In *Proceedings of the 2018 26th ACM Joint Meeting on European Software Engineering Conference and Symposium on the Foundations of Software Engineering*. 257–268.
- [8] Steven Elsworth and Stefan Güttel. 2020. Time Series Forecasting Using LSTM Networks: A Symbolic Approach. *arXiv preprint arXiv:2003.05672* (2020).
- [9] Cristóbal Esteban, Stephanie L Hyland, and Gunnar Rätsch. 2017. Real-valued (medical) time series generation with recurrent conditional gans. *arXiv preprint arXiv:1706.02633* (2017).
- [10] Robert Fortet and Edith Mourier. 1953. Convergence de la répartition empirique vers la répartition théorique. In *Annales scientifiques de l'École Normale Supérieure*, Vol. 70. 267–285.
- [11] Ian Goodfellow, Jean Pouget-Abadie, Mehdi Mirza, Bing Xu, David Warde-Farley, Sherjil Ozair, Aaron Courville, and Yoshua Bengio. 2014. Generative adversarial nets. In *Advances in neural information processing systems*. 2672–2680.
- [12] Alex Graves. 2013. Generating sequences with recurrent neural networks. *arXiv preprint arXiv:1308.0850* (2013).
- [13] Hamed Haddadi. 2010. Fighting online click-fraud using bluff ads. *ACM SIGCOMM Computer Communication Review* 40, 2 (2010), 21–25.
- [14] Ch Md Rakim Haider, Anindya Iqbal, Atif Hasan Rahman, and M Sohail Rahman. 2018. An ensemble learning based approach for impression fraud detection in mobile advertising. *Journal of Network and Computer Applications* 112 (2018), 126–141.
- [15] Martin Heusel, Hubert Ramsauer, Thomas Unterthiner, Bernhard Nessler, and Sepp Hochreiter. 2017. Gans trained by a two time-scale update rule converge to a local nash equilibrium. In *Advances in neural information processing systems*. 6626–6637.
- [16] Wang Jianyu, Wu Chunming, Ji Shouling, Gu Qinchun, and Li Zhao. 2017. Fraud Detection via Coding Nominal Attributes. In *Proceedings of the 2017 2nd International Conference on Multimedia Systems and Signal Processing*. 42–45.
- [17] Kawaljeet Kaur Kapoor, Yogesh K Dwivedi, and Niall C Piercy. 2016. Pay-per-click advertising: A literature review. *The Marketing Review* 16, 2 (2016), 183–202.
- [18] Nathan Killoran, Leo J Lee, Andrew Delong, David Duvenaud, and Brendan J Frey. 2017. Generating and designing DNA with deep generative models. *arXiv preprint arXiv:1712.06148* (2017).
- [19] Sneha Kudugunta and Emilio Ferrara. 2018. Deep neural networks for bot detection. *Information Sciences* 467 (2018), 312–322.
- [20] Laurens van der Maaten and Geoffrey Hinton. 2008. Visualizing data using t-SNE. *Journal of machine learning research* 9, Nov (2008), 2579–2605.
- [21] Riwa Mouawi, Imad H Elhajj, Ali Chehab, and Ayman Kayssi. 2019. Crowdsourcing for click fraud detection. *EURASIP Journal on Information Security* 2019, 1 (2019), 11.
- [22] Shishir Nagaraja and Ryan Shah. 2019. Clicktok: click fraud detection using traffic analysis. In *Proceedings of the 12th Conference on Security and Privacy in Wireless and Mobile Networks*. 105–116.
- [23] Daniel Neil, Michael Pfeiffer, and Shih-Chii Liu. 2016. Phased lstm: Accelerating recurrent network training for long or event-based sequences. In *Advances in neural information processing systems*. 3882–3890.
- [24] Michael Neunert, Abbas Abdolmaleki, Markus Wulfmeier, Thomas Lampe, Jost Tobias Springenberg, Roland Hafner, Francesco Romano, Jonas Buchli, Nicolas Heess, and Martin Riedmiller. 2020. Continuous-Discrete Reinforcement Learning for Hybrid Control in Robotics. *arXiv preprint arXiv:2001.00449* (2020).
- [25] Richard Oentaryo, Ee-Peng Lim, Michael Finegold, David Lo, Feida Zhu, Clifton Phua, Eng-Yeow Cheu, Ghim-Eng Yap, Kelvin Sim, Minh Nhut Nguyen, et al. 2014. Detecting click fraud in online advertising: a data mining approach. *The Journal of Machine Learning Research* 15, 1 (2014), 99–140.
- [26] Alec Radford, Luke Metz, and Soumith Chintala. 2015. Unsupervised representation learning with deep convolutional generative adversarial networks. *arXiv preprint arXiv:1511.06434* (2015).
- [27] Mehdi SM Sajjadi, Olivier Bachem, Mario Lucic, Olivier Bousquet, and Sylvain Gelly. 2018. Assessing generative models via precision and recall. In *Advances in Neural Information Processing Systems*. 5228–5237.
- [28] Kaleb E Smith and Anthony O Smith. 2020. Conditional GAN for timeseries generation. *arXiv preprint arXiv:2006.16477* (2020).
- [29] Richard S Sutton and Andrew G Barto. 2018. *Reinforcement learning: An introduction*. MIT press.
- [30] Kurt Thomas, Juan A Elices Crespo, Ryan Rasti, Jean-Michel Picod, Cait Phillips, Marc-André Decoste, Chris Sharp, Fabio Tirelo, Ali Tofigh, Marc-Antoine Courteau, et al. 2016. Investigating commercial pay-per-install and the distribution of unwanted software. In *25th {USENIX} Security Symposium ({USENIX} Security 16)*. 721–739.
- [31] Shuai Xiao, Junchi Yan, Mehrdad Farajtabar, Le Song, Xiaokang Yang, and Hongyuan Zha. 2017. Joint modeling of event sequence and time series with attentional twin recurrent neural networks. *arXiv preprint arXiv:1703.08524* (2017).
- [32] Lantao Yu, Weinan Zhang, Jun Wang, and Yong Yu. 2017. Seqgan: Sequence generative adversarial nets with policy gradient. In *Thirty-first AAAI conference on artificial intelligence*.
- [33] Pengyu Zhao, Tianxiao Shui, Yuanxing Zhang, Kecheng Xiao, and Kaigui Bian. 2020. Adversarial Oracular Seq2seq Learning for Sequential Recommendation. In *Proceedings of the Twenty-Ninth International Joint Conference on Artificial Intelligence, IJCAI 1905–1911*.
- [34] Panpan Zheng, Shuhan Yuan, Xintao Wu, Jun Li, and Aidong Lu. 2019. One-class adversarial nets for fraud detection. In *Proceedings of the AAAI Conference on Artificial Intelligence*, Vol. 33. 1286–1293.
- [35] Xingquan Zhu, Haicheng Tao, Zhiang Wu, Jie Cao, Kristopher Kalish, and Jeremy Kayne. 2017. *Fraud prevention in online digital advertising*. Springer.
- [36] Yu Zhu, Hao Li, Yikang Liao, Beidou Wang, Ziyu Guan, Haifeng Liu, and Deng Cai. 2017. What to Do Next: Modeling User Behaviors by Time-LSTM.. In *IJCAI*, Vol. 17. 3602–3608.